

Effects of aluminum incorporation on band alignment at the SiO₂/HfO₂ interface

Onise Sharia,¹ Alexander A. Demkov,^{1,*} Gennadi Bersuker,² and B. H. Lee²

¹*Department of Physics, The University of Texas at Austin, Austin, Texas 78712, USA*

²*SEMATECH, Austin, Texas 78741, USA*

(Received 16 August 2007; revised manuscript received 12 November 2007; published 28 February 2008)

A high- k HfO₂/SiO₂ gate stack is taking the place of SiO₂ as a gate dielectric in a modern field effect transistor. The use of HfO₂ requires employing a metal gate electrode that limits available options for controlling transistor threshold voltage by modulating the electrode work function. An alternative approach is to modify the overall band alignment in the gate stack. To guide the experiment in finding a way of engineering the stack composition in order to control the band offset, we investigate theoretically the effects of Al incorporation in the high- k HfO₂/SiO₂ gate stack (effectively, this creates a pseudobinary alloy Al₂O₃-HfO₂). It is shown that O vacancies are stabilized in the vicinity of substitutional Al in the SiO₂ interfacial layer. We find that Al interstitial atoms pair up and form a stable Al-vacancy complex in the vicinity of the HfO₂/SiO₂ interface. Based on a previously introduced model, which suggests that the oxygen depleted interface provides much less effective screening of the interfacial dipole, we show that Al incorporation in the SiO₂ layer may shift significantly the band alignment between hafnia and silica, increasing the band offset by up to 1.8 eV.

DOI: 10.1103/PhysRevB.77.085326

PACS number(s): 73.40.Qv, 71.15.-m, 71.20.-b

INTRODUCTION

HfO₂ and Hf silicates have been recently studied extensively because of their potential application as a gate dielectric in complementary metal oxide semiconductor (CMOS) technology. Due to their higher dielectric constant with respect to SiO₂, Hf-based dielectrics are expected to allow for continuous transistor scaling without compromising device performance.¹ Among other challenges associated with the integration of these novel gate dielectric materials into the standard transistor fabrication process is the requirement to identify metal electrodes, which would exhibit the Si band edge work function values (matching the ones of the n and p types of Si substrate). Due to inherent instability of the metals in contact with hafnia under high temperature processing conditions, the focus is shifted toward developing a metal gate stack with appropriate effective work function, which would provide the required low transistor threshold voltage. This approach includes, among other techniques, incorporation of metal ions in the gate stack by means of the ion diffusion from the thin capping layer deposited on top of the Hf-based dielectric.

High- k gate stacks usually include a thin SiO₂ layer, grown either intentionally or spontaneously, near the interface with the Si substrate.² This thin layer obviously affects the overall band alignment of the Si/SiO₂/HfO₂/metal stack. The band alignment at the Si/SiO₂ interface was studied extensively both theoretically and experimentally, and the valence band offset is established to be approximately 4.2 eV.³ On the other hand, the valence band discontinuity at the HfO₂/SiO₂ interface is found to be process dependent and vary with the degree of the interface oxidation.⁴⁻⁷ In particular, the charge transfer between hafnia and silica and polarization of the Hf-O-Si bonds, which depends on the density of O atoms at the interface, were identified as the critical factors controlling the band alignment.⁵ Introduction of Al near the interface is expected to change the oxygen density and coordination as well as polarizability of the

M-O-Hf layer that may affect the effective work function of the total high- k gate stack.

In this paper, we report a theoretical study of the effect of Al incorporation near the SiO₂/HfO₂ interface on the band alignment of the gate stack. We study the relative thermodynamic stability of the SiO₂/HfO₂ system with Al atoms occupying various possible types of crystal sites, associated changes in the electronic structure, and corresponding band alignment. The rest of the paper is organized as follows. In the next section, we will discuss theoretical models built to describe the interface and provide essential computational details. These are followed by the discussion of thermodynamic stability and band alignment.

THEORETICAL MODEL AND COMPUTATION DETAILS

We describe the HfO₂/SiO₂ oxide stack theoretically using slab geometry, with 24 Å of vacuum added to eliminate spurious slab/slab interactions. We start with a previously studied structure of the interface constructed from β -cristobalite (C9) silica and monoclinic hafnia, which we referred to as m-332 in Ref. 5 (the details on how these structures are generated can be found in that reference). It has the lowest interface energy and the smallest dipole of all interfaces we have studied. Since the goal of the present study is to consider the effects of doping, we double the simulation cell in one lateral direction. To make sure that the cell size is adequate, we perform one calculation with a $2 \times 2 \times 243$ atom cell. The band offset between silica and hafnia is 0.9 eV. The system is stoichiometric; HfO₂ has a stoichiometric surface with vacuum, SiO₂ is Si terminated, and dangling bonds are tied with hydrogen atoms. At the interface, we have one twofold and two threefold oxygen atoms per primitive (not doubled) cell. The overall size of the simulation cell is therefore $10.4 \times 5.2 \times 53.1$ Å³ and it contains 122 atoms. The thickness of HfO₂ layer is 14.9 Å, and of SiO₂ is 14.5 Å. The structure is shown in Fig. 1.

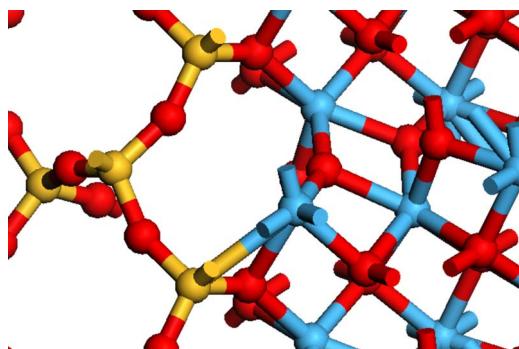


FIG. 1. (Color online) The initial m-332 structure of the $\text{SiO}_2/\text{HfO}_2$ interface (Ref. 5). One can see two threefold oxygen atoms and one twofold that is bonded to hafnia atoms only.

Our calculations are performed within density functional theory^{8,9} in the local density approximation, as implemented in a plane wave basis code VASP.¹⁰ We use the Vanderbilt-type pseudopotential¹¹ for the total energy calculations and projector-augmented-wave (PAW)¹² method to study the site projected density of states. The Ceperley-Adler¹³ exchange-correlation functional is used, as interpolated by Perdew and Zunger.¹⁴ We use the $2 \times 4 \times 1$ Monkhorst-Pack¹⁵ k -point mesh for the integration over the Brillouin zone for the supercell of the size $10 \times 5 \times 53 \text{ \AA}^3$. The total energy change with respect to a finer $4 \times 8 \times 1$ k -point mesh is less than 5 meV per simulation cell. Also, the change of the band alignment for the finer k -point mesh is negligible. The kinetic energy cutoff is 600 eV. The ionic positions are relaxed with the conjugate gradient method with the force tolerance of 0.05 eV/Å.

We have previously shown that changing the coordination of the interfacial oxygen has a strong effect on the band alignment.⁵ This suggests that by reducing the oxygen content at the interface, one might control the offset. One way to achieve this is to introduce a metal with lower oxygen coordination. For example, Si prefers fourfold coordination, Hf prefers eightfold, and octahedral Al is in the middle. This so-called aliovalent doping is often used in ceramics and is usually described in terms of pseudobinary alloys, e.g., $(\text{HfO}_2)_{1-x}(\text{Al}_2\text{O}_3)_x$. Thus, we substitute cations (Si and Hf) with Al while maintaining the overall stoichiometry of the system. This implies removing one oxygen atom for every two Al substitutions. The key element for this strategy is the preferential segregation of Al toward the interface, which as we shall show is indeed the case. Recently, Al has been used to passivate oxygen vacancies in hafnia by creating hafnium aluminate,¹⁶ our strategy is, however, strictly interface specific. Note that this is different from having Al defects. Consider, for example, substituting Si or Hf with Al without introducing charge-compensating oxygen vacancies or interstitials. This would generate holes near the Fermi level, and since in the actual CMOS device the Si Fermi level is above the maximum of the valence bands of both silica and hafnia, the holes (empty levels) would be filled by the substrate electrons. Therefore, we would have a negative charge across the oxide stack. Obviously, this would change the overall band alignment while not contributing to the dipole at the silica/hafnia interface.

To create a simple stoichiometric Al doping model, we substitute two silicon atoms with aluminum (this generates two holes) and compensate this additional +2 charge by removing one oxygen atom. After such substitution, the total number of atoms in the simulation cell is 121. We refer to this structure as V_{Si} . V denotes that there is an oxygen vacancy and the subscript Si denotes that the substitution is in silica. The next step is to identify the energetically preferred geometries. We create three versions of the V_{Si} defect, which differ in the position of the oxygen vacancy: at the interface with hafnia [V_{Si} , Fig. 2(a)], in the first layer from the interface [V_{Si}' , Fig. 2(b)], and in the second layer from the interface [V_{Si}'' , Fig. 2(c)]. We have also considered a possible defect; we substitute only one silicon atom with aluminum and then position aluminum and oxygen atoms interstitially [structure I_{Si} , Fig. 2(d)]. We construct one V_{Hf} -type defect in hafnia with an oxygen vacancy at the interface [Fig. 3(a)] and the interface where both Si and Hf atoms are replaced with Al while one interfacial oxygen is removed [V_{SiHf} , Fig. 3(b)]. After relaxation, the average distance between aluminum and oxygen atoms varies from 1.75 to 1.85 Å compared to 1.86 to 1.96 Å (according to our *ab initio* calculations) in the bulk $\gamma\text{-Al}_2\text{O}_3$. The relaxation does not change the interface structure dramatically except for the case of V_{Si}' , where it results in the formation of a large eight-ring and a small five-ring on the silica side of the interface. This can be attributed to the removal of an oxygen atom from the silica side, which changes the number of atoms in the ring. This is not the case for V_{Si} where the oxygen atom is removed from the interface.

In addition to the interface doping, we also consider Al atoms in the bulk silica and hafnia (V_{SiO_2} and V_{HfO_2}). We calculate three different configurations of defects in silica and two in hafnia. In this study, the total number of atoms in the supercell is 95. The lowest energy defects are shown in Fig. 4. In both cases, the lowest energy is obtained when the oxygen atom, bridging aluminum atoms, is removed. Aluminum atoms move toward each other to minimize the distortion of the structure. In other words, the vacancy is in the first coordination sphere of both Al atoms.

One of the important questions is whether Al atoms located in SiO_2 away from the interface with hafnia affects the band alignment of these materials. To treat the case of non-interfacial doping, we consider supercell geometry in order to avoid possible surface effects caused by the limited size of the simulation cell. We use a $10.38 \times 5.19 \times 42.23 \text{ \AA}^3$ supercell with thicknesses of silica and hafnia being 21.8 and 20.4 Å, respectively. In the case of the Al atoms in silica, we substitute two Si atoms with two Al atoms and create one oxygen vacancy for charge compensation, as discussed in the previous paragraph. The total number of atoms is 167 that results in a rather time consuming calculation. To study Al in hafnia, we use a somewhat smaller cell ($5.19 \times 5.19 \times 42.23 \text{ \AA}^3$). In the following, we refer to the Al in the bulk structures as $V_{\text{SiO}_2}^b$ and $V_{\text{HfO}_2}^b$.

RESULTS AND DISCUSSION

To study the relative stability of the doping configurations, one needs to consider specific chemical reactions.

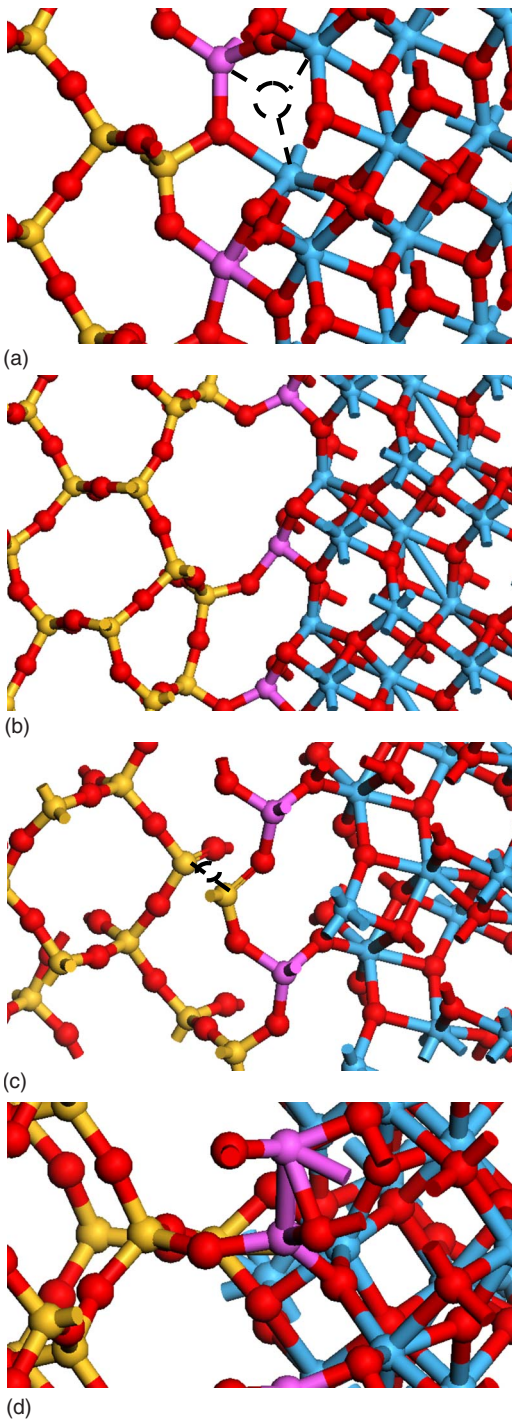


FIG. 2. (Color online) (a) The structure of the doped interface with the V_{Si} complex (see text). The supercell is doubled with respect to m-332. Two silicon atoms are substituted with alumina atoms and one interfacial twofold oxygen atom is removed while the other interfacial oxygen atom remains. The “missing” oxygen atom and bonds are indicated with a dashed circle and lines. (b) The same as the V_{Si} complex, except that the interfacial oxygen atoms are untouched and one oxygen atom from the next layer of oxygen is removed. After the relaxation, the total number of oxygen atoms in the second silica layer is only 3 instead of 4. (c) In this case, an oxygen atom from the third silica layer from the interface is removed. (d) One substitutional and one interstitial aluminum atoms plus one interstitial oxygen atom.

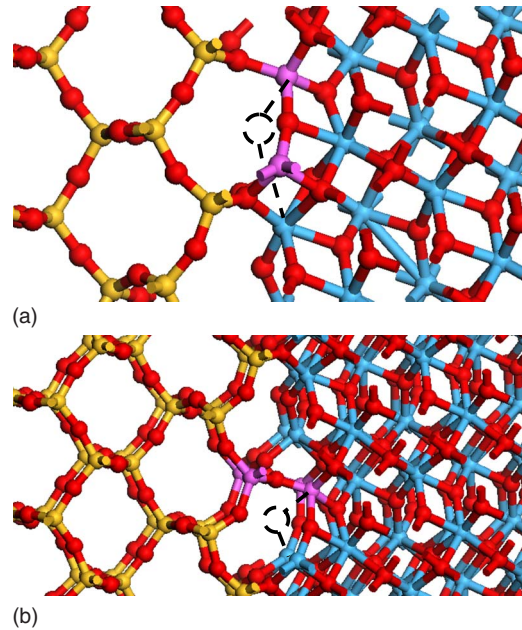


FIG. 3. (Color online) (a) The structure of the doped interface with the V_{Hf} complex (see text). Two hafnia atoms are substituted with aluminum atoms and a twofold interfacial oxygen atom is removed. (b) The structure of the doped interface with the V_{SiHf} complex (see text). One hafnium and one silicon atoms are substituted with two aluminum atoms and an interfacial oxygen atom is removed.

When the number of atoms in two models is the same, it is possible to compare the total energies of two structures. However, when the number of atoms is different, the stability of the defects depends on the chemical environment, and one has to introduce a chemical potential. This procedure is not unique but as long as it is consistent, a meaningful comparison is possible. One of the possible reactions is to bring one Al_2O_3 molecule from bulk Al_2O_3 into SiO_2 , substitute two Si atoms with Al, and remove an oxygen atom. We then assume that these two extra silicon and four oxygen (three from the Al_2O_3 molecule and the one removed) atoms form two SiO_2 molecules in equilibrium with bulk SiO_2 ,

$$\Delta G = E_{V_{\text{Si}}} - E_{\text{m-332}} + E_{\text{SiO}_2} - E_{\text{Al}_2\text{O}_3}.$$

For the V_{SiHf} structure, we consider the formation of a HfSiO_4 molecule. We calculate the bulk structure ($I4_1/amd$ symmetry) of HfSiO_4 (hafnon). Our calculated lattice constants are $a=6.48 \text{ \AA}$ and $c=5.91 \text{ \AA}$, which are 1.5% less than the experimental values.¹⁷ Si-O distance is 1.63 \AA and Hf-O distances are 1.13 and 1.25 \AA . Table I gives the formation energies and the corresponding chemical reactions.

One may consider another reaction by bringing Al, Hf, Si, and O as elements. The free energy difference between any two structures can then be written as

$$\Delta G = \Delta E_{\text{tot}} - \Delta N_{\text{Si}}\mu_{\text{Si}} - \Delta N_{\text{O}}\mu_{\text{O}} - \Delta N_{\text{Al}}\mu_{\text{Al}} - \Delta N_{\text{Hf}}\mu_{\text{Hf}},$$

where the first term describes the change of energy with respect to m-332 (for example, $\Delta E_{\text{tot}}=E_{V_{\text{Si}}}-E_{\text{m-332}}$), Al is considered in equilibrium with a metal source, and we use

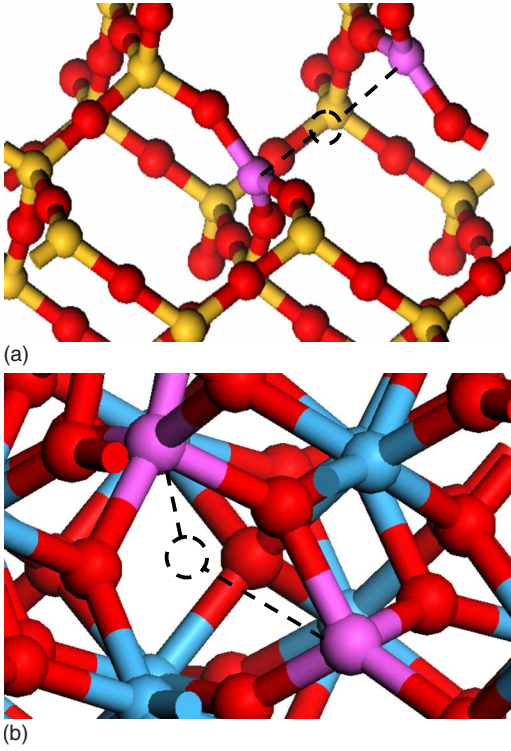


FIG. 4. (Color online) (a) The structure of the doped interface with the V_{SiO_2} complex (see text). The lowest energy structure of a stoichiometric substitution in the bulk SiO_2 . Al substitutes two silicon atoms, and the oxygen atom bridging to alumina sites is removed to create a vacancy. (b) The structure of the doped interface with the V_{HfO_2} complex (see text).

equilibrium conditions for (Si,O) and (Hf,O) pairs with bulk SiO_2 and HfO_2 , respectively. In Fig. 5, we plot the formation energies as a function of the oxygen chemical potential.

Both methods give almost the same estimates of relative stability of different Al complexes. The only discrepancy (of only about 0.2 eV) is the relative stability of I_{Si} vs V_{SiHf} . According to Table II, V_{SiHf} is more stable than I_{Si} , while I_{Si} is more stable according to Fig. 5. Three lowest energy structures are V_{Si} , V_{Si}' , and V_{Hf} , in which V_{Si} has the lowest

TABLE I. The formation energy of different Al doping complexes with respect to the bulk $\gamma\text{-Al}_2\text{O}_3$.

Interface	Reaction	Formation energy (eV)
V_{Si}	$\text{Al}_2\text{O}_3 + \text{m-332} \rightarrow V_{\text{Si}} + 2\text{SiO}_2$	0.38
V_{Si}'	$\text{Al}_2\text{O}_3 + \text{m-332} \rightarrow V_{\text{Si}}' + 2\text{SiO}_2$	0.54
V_{Si}''	$\text{Al}_2\text{O}_3 + \text{m-332} \rightarrow V_{\text{Si}}'' + 2\text{SiO}_2$	7.60
I_{Si}	$\text{Al}_2\text{O}_3 + \text{m-332} \rightarrow I_{\text{Si}} + \text{SiO}_2$	2.90
V_{Hf}	$\text{Al}_2\text{O}_3 + \text{m-332} \rightarrow V_{\text{Hf}} + 2\text{HfO}_2$	0.84
V_{SiHf}	$\text{Al}_2\text{O}_3 + \text{m-332} \rightarrow V_{\text{SiHf}} + \text{SiHfO}_4$	2.65
V_{SiO_2}	$\text{Al}_2\text{O}_3 + \text{m-332} \rightarrow V_{\text{SiO}_2} + 2\text{HfO}_2$	4.67
V_{HfO_2}	$\text{Al}_2\text{O}_3 + \text{m-332} \rightarrow V_{\text{HfO}_2} + 2\text{SiO}_2$	3.24
$V_{\text{SiO}_2}^b$	$\text{Al}_2\text{O}_3 + \text{m-332} \rightarrow V_{\text{SiO}_2}^b + 2\text{HfO}_2$	5.09
$V_{\text{HfO}_2}^b$	$\text{Al}_2\text{O}_3 + \text{m-332} \rightarrow V_{\text{HfO}_2}^b + 2\text{HfO}_2$	3.38

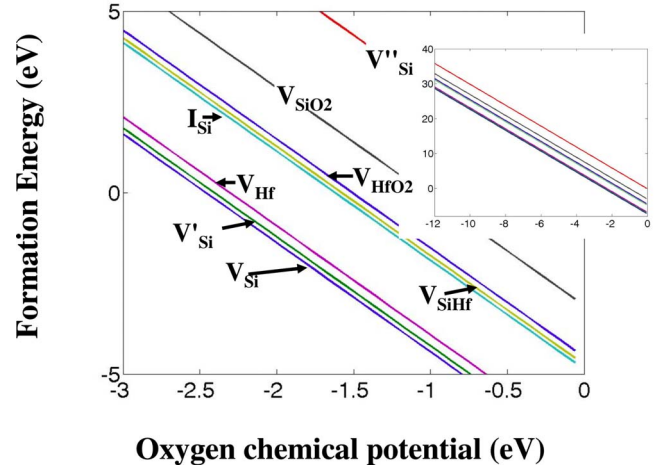


FIG. 5. (Color online) The formation energies of different Al doping complexes versus the chemical potential of oxygen.

energy, and V_{Hf} the highest. This suggests that doping of the silica/hafnia stack occurs via the generation of oxygen vacancies at the interface with hafnia accompanied by the Al substitution (for Si) in silica in the close proximity of the vacancy. Note that the fact that Al prefers to be close to a vacancy is quite general and well known for ceramics. The energy of the vacancy created in the next oxygen layer in silica (with respect to the interface) is slightly higher (V_{Si}'). When an oxygen vacancy is created in the second layer from the interface by removing an O atom to which Al atoms are not connected, the energy is very high (V_{Si}''). In other words, a locally stoichiometric aluminum complex is more stable; this can be viewed as Al pairing. Note that formation energies of V_{Si} and V_{Hf} are similar. Thus, the important conclusion is that Al substitution near the interface is much more preferable thermodynamically than that in the bulk region of either oxide. The exception is the interface V_{Si}'' complex that has a very high energy. Since the formation energy for any vacancy-containing complex near the interface is comparable to the thermal energy at about 1000 °C, one may expect a preferential segregation of Al to the interface. We also observe a slight difference in formation energies between doping bulk silica (V_{SiO_2} complex) and bulklike silica away from the interface ($V_{\text{SiO}_2}^b$). The same is true for doping hafnia (V_{HfO_2} complex) versus bulklike hafnia ($V_{\text{HfO}_2}^b$). However, the difference is very small and does not change the above conclusion.

TABLE II. The valence band offset for different Al-containing interface structures.

Interface	Average potential method (eV)	Projected density of states method (eV)
m-332	0.9	0.7
V_{Si}	-0.2	-0.4
V_{Si}'	0.4	0.2
I_{Si}	0.2	0.2
V_{Hf}	0.3	0.2
V_{SiHf}	-0.9	-1.0

To analyze the valence band offset at the Al-doped $\text{SiO}_2/\text{HfO}_2$, we use two techniques, the average potential method^{18,19} and the density of states analysis.²⁰ Two methods agree with each other within 0.2 eV. While the average potential method provides a unique value for the band discontinuity, the site projected partial density of states analysis gives more detailed information about the valence band maximum, including band bending. The results of the band offset calculations for all structures considered are summarized in Table II. We do not include the structure V_{Si} because it is not insulating and because it has the same problem as nonstoichiometric surfaces. There are unoccupied states in the valence band which would be filled, if a substrate or a gate electrode is included, thus giving additional band shift. We consider this to be an extrinsic effect. All other structures are insulating. As can be seen from Table II, there is a big change in the band alignment with respect to m-332 due to the presence of Al. Note that the change is always one way—the valence band maximum of silica goes up and that of hafnia goes down. The biggest change is 1.8 eV (with respect to the Al-free interface) for the V_{SiHf} structure, which is enough for the valence bands of two oxides to change order. Importantly, Al atoms away from the interface do not affect the alignment as long as the associated vacancy is formed close to Al, which is an energetically preferred configuration.

To ensure that the cell size is adequate, we perform one calculation with a $2 \times 2 \times 243$ atom cell for our V_{SiHf} structure. We considered one Al-vacancy complex. After the relaxation, the formation energy for the complex is 2.4 eV vs 2.6 eV obtained with a $10.38 \times 5.19 \times 53.05 \text{ \AA}^3$ cell, which is reasonably close. The valence band offset is 0.2 eV; thus, the difference with respect to m-332 is 0.7 eV vs 1.8 eV without doubling the cell. In other words, reducing the number of Al atoms by the factor of 2 reduces the effect on the valence band offset by the same factor, as expected. This confirms our results qualitatively and puts an upper bound on the energies of the order of 0.2 eV.

Since the V_{SiHf} structure is so unusual, we now discuss the band alignment in more detail. In Fig. 6 we show the plane-averaged and macroscopically averaged electrostatic potentials across the $\text{SiO}_2/\text{HfO}_2$ junction. The calculations of the bulk structures of silica and hafnia place the maxima of their valence bands at -2.7 and -3.6 eV, respectively. This results in a 0.9 eV valence band offset, which represents a very large change with respect to the initial (Al-free) m-332 structure. We determine the positions of the conduction band minima using experimental values for the band gaps, 9.0 eV (Ref. 21) for silica and 5.7 eV (Ref. 22) for hafnia. This gives us a -4.2 eV conduction band discontinuity. A small electric field can be seen across the vacuum layer in Fig. 6. Using the experimental value for the HfO_2 band gap, its electron affinity comes out around 1.9 eV based on our results, in good agreement with the recent measurement of Sayan *et al.*⁴ Since the maximum of the oxide valence band is predominantly derived from the oxygen p states, one can track the variation in the valence band edge across the heterojunction by tracking these states. In Fig. 7, we plot the partial density of states projected onto p states of oxygen atoms in each atomic plane (parallel to the interface) as a function of the depth across the V_{SiHf} structure. The Fermi

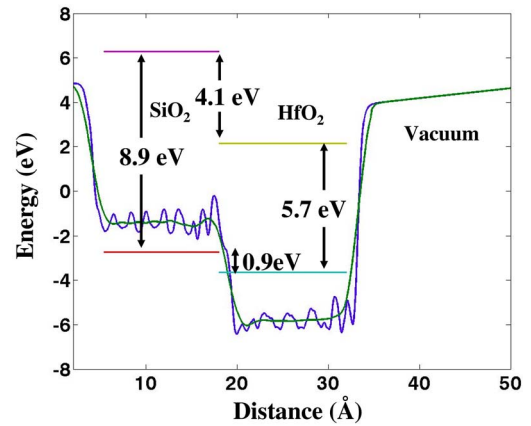


FIG. 6. (Color online) The plane-averaged electrostatic potential for the V_{Si} interface. The average values for the potential in the bulk silica and hafnia are used to determine the positions of the valence band maxima in silica and hafnia. Experimental band gap values are used to place the corresponding conduction band edges.

level is set to zero energy. In HfO_2 , there is some ambiguity to which layer a given oxygen atom belongs to. For clarity and plotting convenience, we combine two layers of oxygen atoms in the hafnia side. As can be seen, Al bonded states extend into bulk for two layers on both sides of the interface (in the graph, each panel on the hafnia side represents two layers). Also, the relative height of the Al-related peaks in hafnia is smaller because the number of oxygen atoms in a layer in hafnia is twice that in silica (the relative number of atoms bonded to Al is smaller). The energies of the valence band maximum of both silica and hafnia away from the interface converge rapidly to the corresponding bulk values, with practically no band bending. In this case, the average potential method agrees well with the partial DOS analysis. Note that there are two types of oxygen atoms in the interface region, those bonded to Al and those not. To identify the band edge, we include only those oxygen atoms, which are

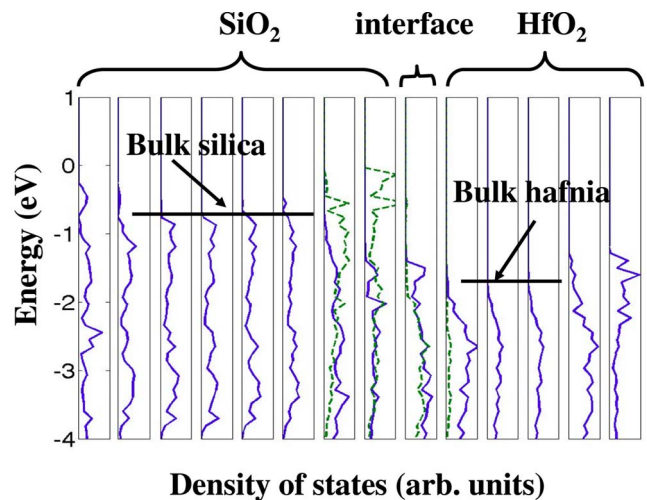


FIG. 7. (Color online) The partial density of states site projected onto the oxygen p state and plotted plane by plane (see text) as a function of depth across the $\text{SiO}_2/\text{HfO}_2$ slab for the V_{SiHf} structure. The dashed lines correspond to oxygen atoms directly bonded to Al.

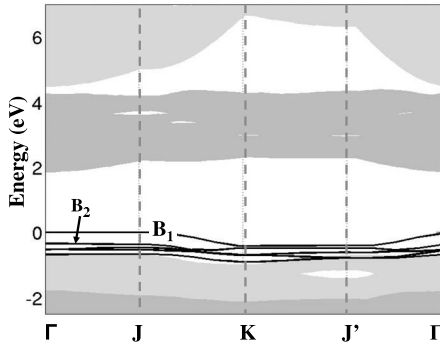


FIG. 8. The interface band structure for the junction with the V_{SiHf} complex.

not bonded to aluminum. The density of states corresponding to oxygen atoms bonded to aluminum is shown as a dashed line. Note that the “defect” states decay rapidly into the bulk of each oxide.

In Fig. 8, we plot the interface band structure for the V_{SiHf} junction. The lighter shaded area represents the band structure of bulk silica, and the darker shaded area that of bulk hafnia. The Fermi level is set at zero energy. There are several occupied flat bands above the valence band maximum of silica. In order to identify the origin of these states, in Fig. 9, we plot the planar averaged charge density for the two highest occupied bands (B_1 and B_2) as a function of z . One can see that band B_1 is localized at the interface, while band B_2 is localized mainly at the free SiO_2 surface. Other bands in Fig. 8 located above the valence band maximum of silica are also localized at the surface of silica. This is in agreement with the partial density of states plot: the highest occupied level is derived from the interface which is 0.35 eV above the surface states of silica. The B_1 band was not present in the m-332 structure. It is pinning the Fermi level approximately 0.5 eV above the maximum of the SiO_2 valence band. The charge distribution of B_1 is not symmetric with respect to the interfacial layer (the position of the interface is defined by the position of the oxygen atom connecting two aluminum atoms). This asymmetry reflects the charge transfer from

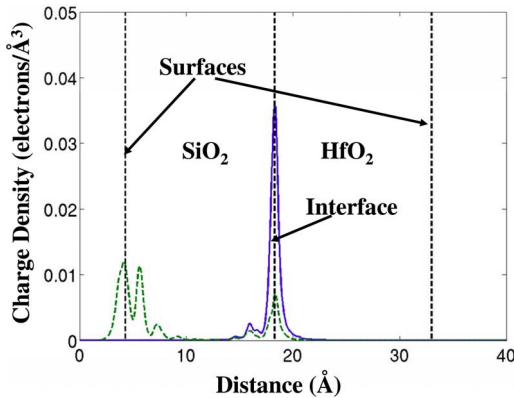


FIG. 9. (Color online) The charge density distribution for the interface B_1 (solid line) and silica surface B_2 (dashed line) bands of the V_{SiHf} structure.

hafnia to silica. We calculate the total charge density on the left and right of the interface and find that the difference is $0.004 e/\text{Å}^2$. There are more electrons on the silica side than on the hafnia side. This creates a positive charge in hafnia. Using a plane capacitor model, the potential drop in the dipole layer is

$$\Delta V = \frac{d\sigma}{\epsilon_0},$$

where d is the thickness of the dipole layer, if we take it to be 3 Å (the distance between Al atoms) that results in a 2.0 eV change in the band alignment vs 1.8 eV in Table II. Obviously, there is room for speculation for the value of d but within a reasonable range, it gives a qualitatively correct estimate.

Qualitatively, our *ab initio* results can be explained in the following way. In the case of noninteracting oxide layers, their band offset is described by the Schottky equation (the difference in electron affinities—the so-called Schottky limit). When the oxides are brought in contact, the charge transfer between the materials takes place, leading to a dipole formation across the interface. The associated electric field results in a correction to the Schottky limit of the band alignment. This dipole is formed by the Si-O-Hf bridge due to the difference in the electronegativity between Si and Hf (alternatively, it can be seen as a result of the difference in electron affinities of two oxides). This dipole is then partially screened by the polarization of the interfacial oxygen atoms, which minimizes the total dipole effect.⁵ In the relaxed m-332 structure, the substitution of two Si with two Al [note that the electronegativity of Al (1.61) is between that of Si (1.9) and Hf (1.3)] and the removal of an interfacial oxygen atom reduces the contribution of the oxygen polarizability to the screening of the interfacial dipole that results in the stronger deviation of the band alignment from the Schottky limit. (This analysis does not apply directly to the I_{Si} structure where we consider interstitial Al and oxygen. Thus, the dielectric screening would actually increase. However, we also increase the number of electronegative metal atoms which would increase the charge transfer.) To summarize our argument, Al doping forces the system to reduce its interface oxygen content (one Si needs two oxygen atoms but one Al needs only three-halves) primarily at the silica/hafnia interface, resulting in a large interface dipole and a sizable increase of the band offset.

CONCLUSIONS

We report a theoretical study of the effects of Al doping of the $\text{SiO}_2/\text{HfO}_2$ heterostructure and, in particular, on the change in the band alignment caused by the interaction between the materials in the presence of Al impurities. Our calculations suggest that Al tends to accumulate near the

SiO₂/HfO₂ interface, simultaneously reducing the amount of oxygen in that region. According to the model, this oxygen is responsible for screening the interfacial dipoles formed due to the charge transfer between the materials with different electronegativities. Thus, higher oxygen deficiency of the interfacial region leads to an increase of the effect of the interface dipole on band alignment, shifting it away from the Schottky limit. We find that Al in the SiO₂ layer near its interface with HfO₂ changes the band discontinuity signifi-

cantly, thus offering a way to adjust the overall band alignment in the stack.

ACKNOWLEDGMENTS

This work was supported by the National Science Foundation under Grant No. DMR-0548182 and Texas Advances Computing Center. We thank John Robertson and S. C. Song for insightful discussions.

*demkov@physics.utexas.edu

- ¹G. D. Wilk, R. M. Wallace, and J. M. Anthony, *J. Appl. Phys.* **89**, 5243 (2001).
²D. Triyoso, R. Liu, D. Roan, M. Ramon, N. V. Edwards, R. Gregory, D. Werho, J. Kulik, G. Tam, E. Irwin, X.-D. Wang, L. B. La, C. Hobbs, R. Garcia, J. Baker, B. E. White, Jr., and P. Tobin, *J. Electrochem. Soc.* **151**, F220 (2004).
³T. Hattori, *Crit. Rev. Solid State Mater. Sci.* **204**, 339 (1995).
⁴S. Sayan, E. Grafunkel, and S. Suzer, *Appl. Phys. Lett.* **80**, 2135 (2002).
⁵O. Sharia, A. A. Demkov, G. Bersuker, and B. H. Lee, *Phys. Rev. B* **75**, 035306 (2007).
⁶J. L. Gavartin and A. L. Schluger, *Microelectron. Eng.* **84**, 2412 (2007).
⁷R. Chau, *IEEE Electron Device Lett.* **25**, 408 (2004).
⁸P. Hohenberg and W. Kohn, *Phys. Rev.* **136**, B864 (1964).
⁹W. Kohn and L. J. Sham, *Phys. Rev.* **140**, A1133 (1965).
¹⁰G. Kresse and J. Furthmuller, *Phys. Rev. B* **54**, 11169 (1996); *Comput. Mater. Sci.* **6**, 15 (1996); G. Kresse and J. Hafner,

- Phys. Rev. B* **47**, RC558 (1993); **48**, 13115 (1993); **49**, 14251 (1994); *J. Phys.: Condens. Matter* **6**, 8245 (1994).
¹¹D. Vanderbilt, *Phys. Rev. B* **41**, 7892 (1990).
¹²P. E. Blöchl, *Phys. Rev. B* **50**, 17953 (1994).
¹³D. M. Ceperley and B. J. Alder, *Phys. Rev. Lett.* **45**, 566 (1980).
¹⁴J. P. Perdew and A. Zunger, *Phys. Rev. B* **23**, 5048 (1981).
¹⁵H. J. Monkhorst and J. D. Pack, *Phys. Rev. B* **13**, 5188 (1976).
¹⁶Q. Li, K. M. Koo, W. M. Lau, P. F. Lee, J. Y. Dai, Z. F. Hou, and X. G. Gong, *Appl. Phys. Lett.* **88**, 182903 (2006).
¹⁷J. A. Speer and B. Cooper, *Am. Mineral.* **67**, 804 (1982).
¹⁸D. M. Bylander and L. Kleinman, *Phys. Rev. B* **36**, 3229 (1987).
¹⁹C. G. Van de Walle, *Phys. Rev. B* **39**, 1871 (1989).
²⁰A. A. Demkov, R. Liu, X. Zhang, and H. Loechelt, *J. Vac. Sci. Technol. B* **18**, 2388 (2000).
²¹T. H. DiStefano and D. E. Eastman, *Solid State Commun.* **9**, 2259 (1971).
²²M. Balog, M. Schieber, M. Michiman, and S. Patai, *Thin Solid Films* **41**, 247 (1977).